Light trapping in ultrathin silicon photonic crystal superlattices with randomly-textured dielectric incouplers

Dennis M. Callahan,[1,*] Kelsey A. W. Horowitz,[1] and Harry A. Atwater[1]

[1]*Thomas J. Watson Lab. of Applied Physics, MS 128-95, California Institute of Technology, Pasadena, CA 91125, USA*

[*]*callahan@caltech.edu*

Abstract: We report here several different superlattice photonic crystal based designs for 200nm thick c-Si solar cells, demonstrating that these structures have the ability to increase broadband absorption from λ = 300nm to 1100nm by more than 100% compared to a planar cell with an optimized anti-reflection coating. We show that adding superlattices into photonic crystals introduces new optical modes that contribute to enhanced absorption. The greatest improvements are obtained when combining a superlattice photonic crystal with a randomly textured dielectric coating that improves incoupling into the modes of the absorbing region. Finally, we show that our design methodology is also applicable to layers 1 to 4 microns in thickness, where absorbed currents competitive with conventional thick Si solar cells may be achieved.

OCIS codes: (350.4238) Nanophotonics and photonic crystals; (350.6050) Solar energy; (050.5298) Photonic crystals.

References and links

1. D. M. Callahan, J. N. Munday, and H. A. Atwater, "Solar cell light trapping beyond the ray optic limit," Nano Lett. **12**(1), 214–218 (2012).
2. Z. Yu, A. Raman, and S. Fan, "Fundamental limit of nanophotonic light trapping in solar cells," Proc. Natl. Acad. Sci. U. S. A. **107**(41), 17491–17496 (2010).
3. E. Garnett and P. Yang, "Light trapping in silicon nanowire solar cells," Nano Lett. **10**(3), 1082–1087 (2010).
4. M. D. Kelzenberg, S. W. Boettcher, J. A. Petykiewicz, D. B. Turner-Evans, M. C. Putnam, E. L. Warren, J. M. Spurgeon, R. M. Briggs, N. S. Lewis, and H. A. Atwater, "Enhanced absorption and carrier collection in Si wire arrays for photovoltaic applications," Nat. Mater. **9**(3), 239–244 (2010).
5. J. Grandidier, D. M. Callahan, J. N. Munday, and H. A. Atwater, "Light absorption enhancement in thin-film solar cells using whispering gallery modes in dielectric nanospheres," Adv. Mater. **23**(10), 1272–1276 (2011).
6. J. Zhu, C. M. Hsu, Z. F. Yu, S. H. Fan, and Y. Cui, "Nanodome solar cells with efficient light management and self-cleaning," Nano Lett. **10**(6), 1979–1984 (2010).
7. P. Bermel, C. Luo, L. Zeng, L. C. Kimerling, and J. D. Joannopoulos, "Improving thin-film crystalline silicon solar cell efficiencies with photonic crystals," Opt. Express **15**(25), 16986–17000 (2007).
8. A. Chutinan and S. John, "Light trapping and absorption optimization in certain thin-film photonic crystal architectures," Phys. Rev. A **78**(2), 023825 (2008).
9. H. A. Atwater and A. Polman, "Plasmonics for improved photovoltaic devices," Nat. Mater. **9**(3), 205–213 (2010).
10. C. Wang, S. Yu, W. Chen, and C. Sun, "Highly efficient light-trapping structure design inspired by natural evolution," Sci. Rep. **3**, 1025 (2013).
11. C. Battaglia, C. M. Hsu, K. Söderström, J. Escarré, F. J. Haug, M. Charrière, M. Boccard, M. Despeisse, D. T. L. Alexander, M. Cantoni, Y. Cui, and C. Ballif, "Light trapping in solar cells: can periodic beat random?" ACS Nano **6**(3), 2790–2797 (2012).
12. V. E. Ferry, M. A. Verschuuren, M. C. Lare, R. E. I. Schropp, H. A. Atwater, and A. Polman, "Optimized spatial correlations for broadband light trapping nanopatterns in high efficiency ultrathin film a-Si:H solar cells," Nano Lett. **11**(10), 4239–4245 (2011).
13. M. Peters, K. Forberich, C. Battaglia, A. G. Aberle, and B. Blasi, "Comparison of periodic and random structures for scattering in thin-film microcrystalline silicon solar cells," Proc. SPIE **8438**, 84380F (2012).

#196231 - $15.00 USD Received 22 Aug 2013; revised 5 Nov 2013; accepted 21 Nov 2013; published 3 Dec 2013

14. C. X. Lin and M. L. Povinelli, "Optimal design of aperiodic, vertical silicon nanowire structures for photovoltaics," Opt. Express **19**(S5), A1148–A1154 (2011).
15. C. X. Lin, N. F. Huang, and M. L. Povinelli, "Effect of aperiodicity on the broadband reflection of silicon nanorod structures for photovoltaics," Opt. Express **20**(S1), A125–A132 (2012).
16. K. Vynck, M. Burresi, F. Riboli, and D. S. Wiersma, "Photon management in two-dimensional disordered media," Nat. Mater. **11**(12), 1017–1022 (2012).
17. E. Yablonovitch and G. D. Cody, "Intensity enhancement in textured optical sheets for solar-cells," IEEE Trans. Electron. Dev. **29**(2), 300–305 (1982).
18. P. Sheng, A. N. Bloch, and R. S. Stepleman, "Wavelength-selective absorption enhancement in thin-film solar cells," Appl. Phys. Lett. **43**(6), 579–581 (1983).
19. H. Altug and J. Vuckovic, "Two-dimensional coupled photonic crystal resonator arrays," Appl. Phys. Lett. **84**(2), 161–163 (2004).
20. A. Yariv, Y. Xu, R. K. Lee, and A. Scherer, "Coupled-resonator optical waveguide: a proposal and analysis," Opt. Lett. **24**(11), 711–713 (1999).
21. H. Altug, D. Englund, and J. Vuckovic, "Ultrafast photonic crystal nanocavity laser," Nat. Phys. **2**(7), 484–488 (2006).
22. J. Ma, L. J. Martínez, and M. L. Povinelli, "Optical trapping via guided resonance modes in a Slot-Suzuki-phase photonic crystal lattice," Opt. Express **20**(6), 6816–6824 (2012).
23. K. X. Wang, Z. Yu, V. Liu, Y. Cui, and S. Fan, "Absorption enhancement in ultrathin crystalline silicon solar cells with antireflection and light-trapping nanocone gratings," Nano Lett. **12**(3), 1616–1619 (2012).

1. Introduction

The cost per watt of photovoltaic modules has been steadily decreasing due to increased manufacturing capacity. Currently, the cost of the wafer is one of the dominant expenses for a photovoltaic cell, and thus engineering efficient thin film devices has the potential to significantly reduce cost. Inherently, the short collection lengths in thin film devices can lead to improved open circuit voltage and relaxed material constraints in cells with very low surface recombination velocities. However, thin films suffer from poor light absorption, and advanced light trapping strategies are required for these cells to achieve reasonable efficiencies and competitive cells.

Nanostructured photovoltaics are an attractive possible solution to this problem. Texturing the active layer of a solar cell on a wavelength scale has recently been shown to have potential to exceed the traditional ray optic light trapping limit [1, 2]. This is due to the fact that a properly nanostructured device can have an elevated local density of optical states (LDOS) throughout the absorber region, increasing the light matter interaction and allowing the possibility for more energy to be coupled into the solar cell where it can be absorbed. There are numerous ways to nanostructure a photovoltaic absorber layer that have been explored recently including the use of nanowires [3, 4], nanospheres [5], nanodomes [6], photonic crystals [7, 8], and plasmonic structures [9]. While it has been shown in numerous publications [1, 2, 10] that the ray optic limit can be exceeded in low index polymer materials, it is much more challenging to achieve maximum light trapping in thin films of high index materials such as Si, where more work is needed.

A major open question in nanophotonic light trapping is whether periodic, aperiodic or a random texturing is optimum [11–13]. There are many different ways to explore the design space between periodic and random, including adding randomness to the absorber, incoupler, or both. Previous work has focused on tuning disorder in the absorber. In one study, a random walk algorithm was used to optimize the lattice positions of Si nanowires, and it was found that aperiodic lattices outperformed periodic ones [14]. Further studies proved that too much randomness decreased absorption [15]. Recent work with air holes in thin Si slabs has also shown that a proper degree of "randomness" designed using structural correlations outperformed an uncorrelated random lattice [16].

We approach this question by considering separately the two most important factors regarding light trapping [1, 17]: incoupling and the density of optical states. An optimal light trapping structure will have a large density of optical states within the absorber, as well as the ability to fully populate all of the optical modes of the device (i.e. maximize the modal occupation number for each mode). Traditionally, for a bulk absorbing material, the optimal

#196231 - $15.00 USD Received 22 Aug 2013; revised 5 Nov 2013; accepted 21 Nov 2013; published 3 Dec 2013

light trapping structure has been a random, Lambertian surface [17]. In this case the density of optical states has been assumed to be that of a homogeneous material with a given refractive index. For a thin film, nanophotonic solar cell, though, this is no longer the case. The density of optical states can actually be increased above that of the bulk, homogeneous value, and thus the limits to absorption can potentially be larger in a nanophotonic solar cell compared to those of a traditional, bulk cell. However, optimal incoupling becomes an issue with thin devices as typical Lambertian texturing is usually not possible because it typically requires fabrication of features larger than the thickness of the cell.

Wavelength-scale periodic structures can take advantage of the inherent increases in the density of optical states associated with the periodicity [18], but always come with a significant angular tradeoff that limits the population of optical modes to those which conserve momentum. Ideal random texturing will allow full population of optical modes at all incident angles, but typically does not increase the density of optical states. We have begun exploring these concepts using as a test system a silicon photonic crystal slab that is a weakly absorbing material. We suggest that the optimal light trapping structural motif may exist between the two extremes of perfectly periodic and fully random structures, for the reasons discussed above. This is shown schematically in Fig. 1.

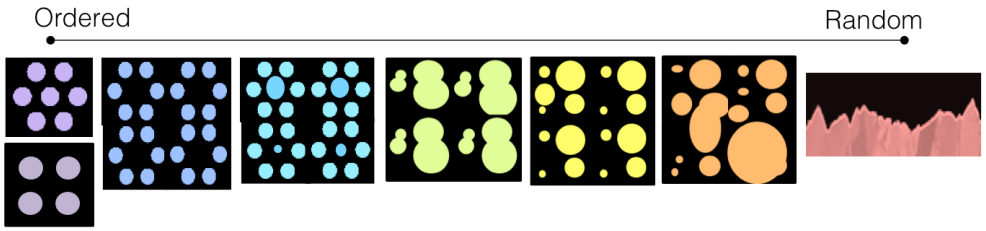

Fig. 1. Conceptual diagram illustrating a range of possible light trapping structures incorporating different degrees of randomness and order.

In this work, we begin with simple periodic two-dimensional slab photonic crystals and begin to add more complexity to them by adding sublattices of "defects" to form 2D photonic crystal superlattices (not to be confused with superlattices of layered semiconductor materials sometimes used in solar cells). This is an initial step away from the leftmost extreme case shown in Fig. 1. These structures perturb the initial periodicity of the traditional photonic crystal structures and introduce new modes into the slab. These modes can act as either localized, isolated resonator modes or as delocalized, Bloch modes formed by infinite coupling of single resonators [19, 20]. Some lattices of this type have been investigated for use in various nano-optics applications such as photonic crystal lasers [21], but not for solar cells. We find that many different superlattice configurations lead to increased absorption compared to simpler photonic crystal lattices. Lastly, for the first time we combine roughened or "random" surfaces with photonic crystals with optimized superlattices to obtain a synergistic effect.

2. Superlattices in a square photonic crystal

Let us first consider a simple square lattice of air holes in Si with a = 290nm and r = 116 nm. We first calculated the normal incidence absorption spectra for this structure and integrated over the AM 1.5 spectrum to obtain an absorbed current. Our calculations are done using rigorous coupled wave analysis (RCWA) using the RSoft DiffractMOD software package and are supported with finite difference time domain (FDTD) calculations using the Lumerical software package.

The normal incidence absorption spectra is shown in Fig. 2. Shown for comparison are the absorption spectra for a 200 nm slab of planar Si with and without an optimized 2-layer anti-

#196231 - $15.00 USD Received 22 Aug 2013; revised 5 Nov 2013; accepted 21 Nov 2013; published 3 Dec 2013

reflection coating. It is interesting to note that even this lattice, which is not optimized, has significantly higher absorption than equivalent thickness planar layers. This simple photonic crystal lattice has a few peaks of high absorption as well as broad wavelength ranges in the solar spectrum where absorption is very weak. The broader peaks are due to Fabry-Perot modes related to the thickness of the slab and the narrower peaks are due to coupling to gamma-point modes of the photonic crystal bandstructure, their number and position dictated by momentum conservation. In the regions where there are no peaks, the lack of absorption is due to either a lack of available optical modes at those frequencies or the inability to couple to these modes from free space, due to momentum conservation. In the present work, we aim to increase the number of these absorption peaks by modifying the original lattice with superlattices of different configurations.

There are numerous ways to introduce superlattices into this structure. We explore four different superlattices which we term “center close-packed,” “center extended,” “edge close-packed,” and “edge extended” as shown in Fig. 3. The terminology is based on the placement and spacing of the “defects” that are introduced to the background lattice. We vary the diameter of the air holes at the superlattice positions and plot the spectral absorption in Fig. 3. For reference, on each of these plots is a vertical dotted white line corresponding to the case when the superlattice air hole diameter is the same as the background lattice (i. e. when the structure is just the original, unperturbed lattice). For each of these superlattices, it can be seen that as soon as the superlattice air holes are different from the background lattice new resonances appear in some regions of the spectrum.

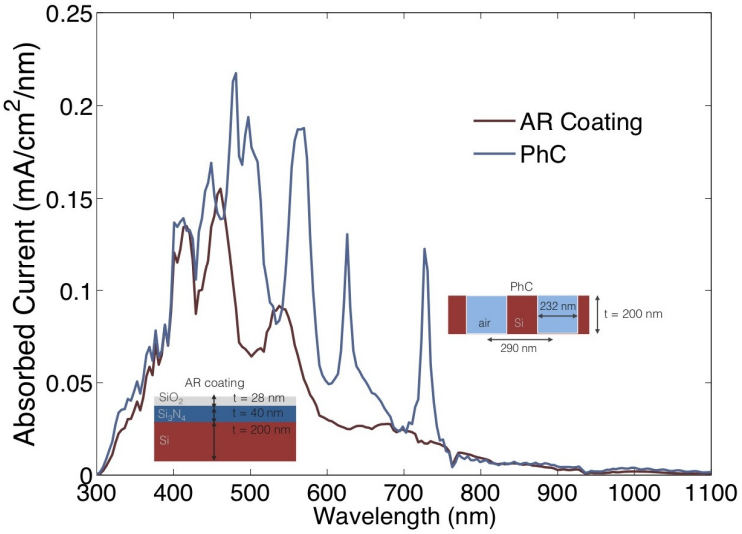

Fig. 2. Absorption spectrum of a planar Si layer with a two-layer AR coating of SiO_2 and Si_3N_4, optimized for thickness, compared to that of a rectangular lattice photonic crystal (r = 116nm, a = 290nm) of the same thickness.

When these absorption spectra are integrated and weighted by the solar spectral flux, we obtain values for total absorbed current as a function of superlattice air hole diameter, shown in Fig. 4. It can be seen that for nearly every defect size in each of the four defect configurations the absorbed current is higher than the original lattice. This corresponds well with the observation of new resonances being introduced when the original lattice is perturbed. The overall absorbed current is a complicated function of where each resonance is introduced into the spectrum and how much current is available in each region. It is interesting to note that for most superlattice diameters the absorbed current increases, but for some diameters it decreases. This is a complicated function of the nature of the newly

#196231 - $15.00 USD Received 22 Aug 2013; revised 5 Nov 2013; accepted 21 Nov 2013; published 3 Dec 2013

introduced modes, where their electric fields are concentrated, Si filling fraction, etc. For each of these lattices, the most resonances and highest integrated absorption occurs for a defect diameter of zero, or when there is no air hole at all at the superlattice locations.

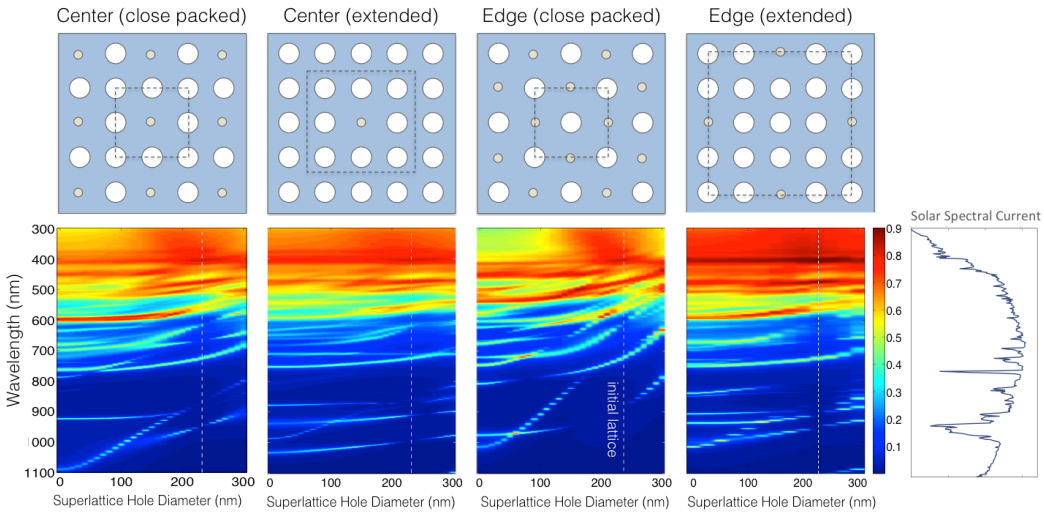

Fig. 3. Four different superlattice geometries (top) and their spectral absorption as a function of superlattice air hole diameter (bottom). For reference, the vertical dotted white lines indicate when the superlattice air hole diameter is the same as the background lattice air hole diameter (i.e. no superlattice).

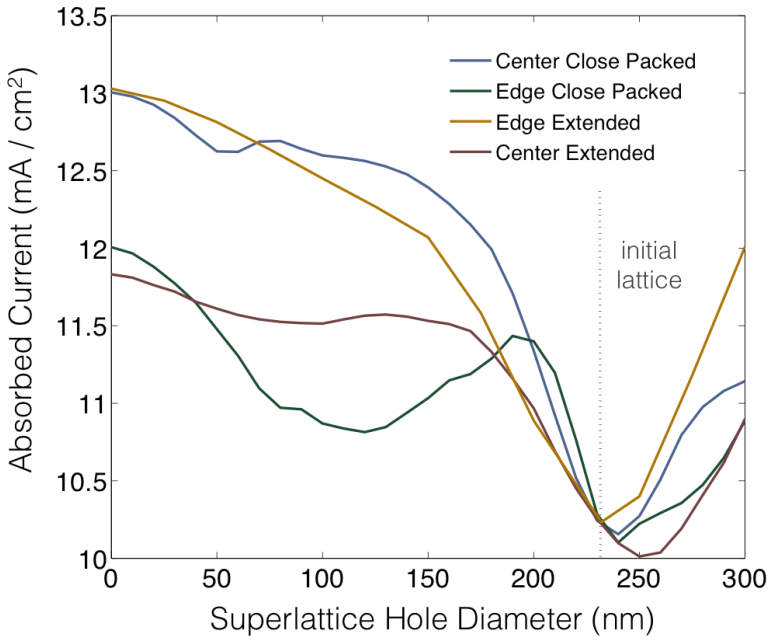

Fig. 4. Absorbed current as a function of superlattice air hole diameter for four different configurations obtained by integrating the spectral absorption data in Fig. 3 and weighting by the AM 1.5 solar spectral current.

To examine the absorption enhancement in further detail, we first take the "center close-packed" lattice with an air hole diameter of 0 nm and plot field profiles in Fig. 5. Figure 5b

#196231 - $15.00 USD Received 22 Aug 2013; revised 5 Nov 2013; accepted 21 Nov 2013; published 3 Dec 2013

shows the electric and magnetic field magnitudes at a wavelength of 678 nm for the original, unperturbed lattice. For comparison, the field magnitudes are also shown in Fig. 5c for the same wavelength with slightly smaller diameter (190 nm) air holes in the superlattice. There is a significantly higher field magnitude for both the electric and magnetic components, as well as different field profiles. The altered field profiles suggest that new optical modes are introduced by the presence of the superlattice. The increased field magnitude leads to the higher absorption than the case without the superlattice. Also worth nothing with these field profiles is the fact that the new modes appear to be extended modes rather than isolated "defect" resonances. This is likely as the locations of the new "defect" air holes are reasonably close, and any mode that would exist inside one of these holes would couple with a neighboring mode, forming a periodic set of coupled resonators analogous to the tight binding description of bound states in solid-state physics.

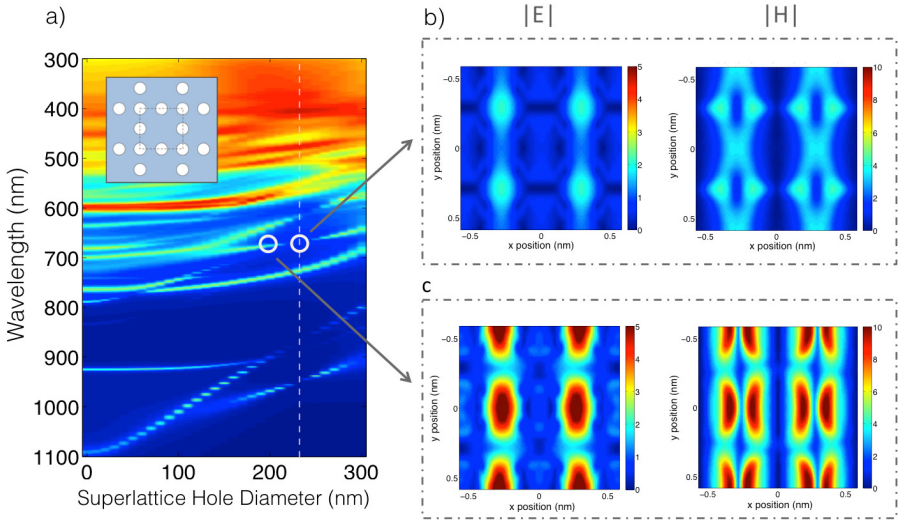

Fig. 5. Field profiles (E-field polarized along y direction) for a wavelength of 678nm for (b) the original lattice and (c) the "center close-packed" superlattice. The field intensities are much higher for the superlattices, leading to increased absorption. The shape of the field profiles is also different in each case, suggesting the introduction of new optical modes through the addition of a superlattice.

Next we examine field profiles from a lattice that has a larger separation between superlattice points, the "edge extended" lattice. Figure 6 shows field profiles for modes at a wavelength at 1010 nm with a superlattice air hole diameter of 0 nm and for the original lattice. Again, it can be seen that the field magnitudes are much higher for the case with the superlattice, leading to the higher absorption at this wavelength. The field profiles are also very different for each case. Here, the fields for the superlattice case are more isolated than for the "center close-packed" lattice, acting more like weakly interacting resonators. This is because the superlattice positions are separated by a larger distance and their resonant field profiles overlap less with neighboring resonators.

#196231 - $15.00 USD Received 22 Aug 2013; revised 5 Nov 2013; accepted 21 Nov 2013; published 3 Dec 2013

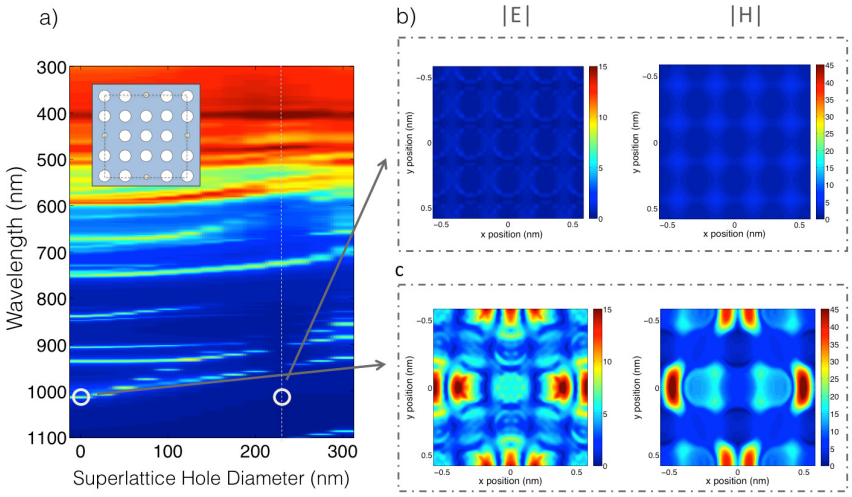

Fig. 6. Field profiles (E-field polarized along y direction) at a wavelength of 1010nm for (b) the original lattice and (c) the "edge-extended" superlattice. In this case, the localized field profiles suggest that the new modes of the superlattice act more like isolated resonators.

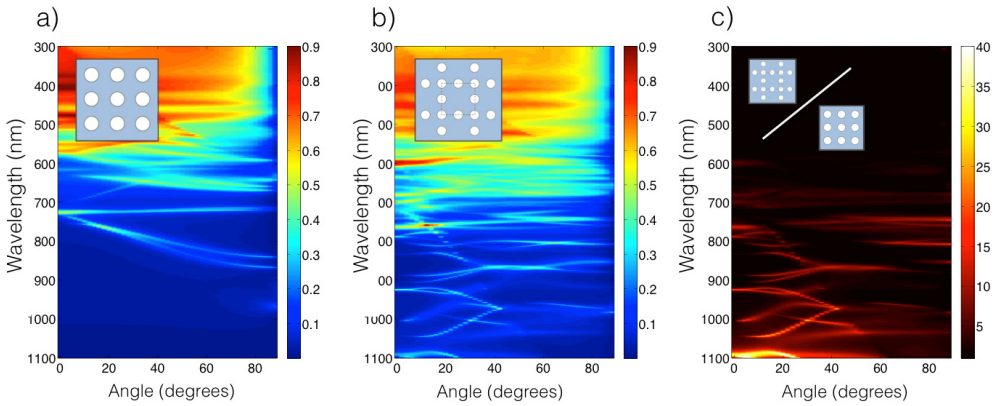

Fig. 7. TE-TM averaged angular absorption spectra for (a) the original lattice, and (b) the "center close-packed" superlattice. (c) Absorption enhancement ratio obtained by dividing spectra (a) by spectra (b).

In Fig. 7 we compare the TM-TE averaged angular spectra for the original lattice and the angular spectra for the "center close-packed" superlattice that has a superlattice air hole diameter of 0 nm. Additional resonances introduced by the superlattice are present at all angles contributing to increased absorption. The fact that they strongly shift in frequency with angle suggests that the defects in this case are coupled together as mentioned above, forming an in-plane coupled resonator waveguide [20] with its own dispersion characteristics. We also plot the absorption enhancement ratio for these two cases in Fig. 7c, which gives a clear map of all the new resonances introduced by the superlattice. In addition to the new resonances introduced by the defects, incoupling to many of the modes present in the simple periodic photonic crystal are altered in the superlattice, as can be seen by the enhanced absorption for the superlattice even for some modes that were also present in the simple periodic photonic crystal. This altered incoupling to the modes of the simple periodic crystal structure could be due to altered reflectivity or through altered scattering due to the change in local dielectric environment. The integrated absorbed current as a function of angle for the initial periodic

#196231 - $15.00 USD Received 22 Aug 2013; revised 5 Nov 2013; accepted 21 Nov 2013; published 3 Dec 2013

case and the structure with an optimal superlattice is shown in Fig. 8. The optimal superlattice always has a higher absorbed current at all angles.

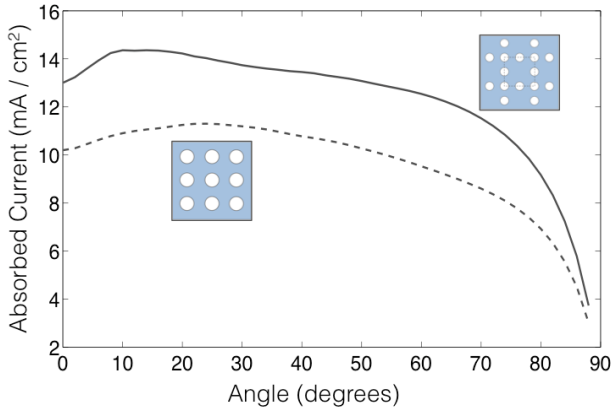

Fig. 8. Integrated absorbed current for the "center close-packed" superlattice (solid line) and the original lattice (dashed line) as a function of incident angle, averaged over TE and TM modes and weighted by the AM 1.5 solar spectral current.

The angular spectra in Fig. 7 shows the modes of the photonic crystal that are accessible from free space, or above the light line. There are other modes within the photonic crystal though that are below the light line and not accessible from free space. To get an idea of how many of these modes there are in each structure, we perform two-dimensional simulations of each structure, injecting energy into each lattice with sets of dipole sources with random positions and phases. We than take the spatial Fourier transform of the resulting field patterns to obtain a reciprocal space representation of the modes excited at each frequency. Upon averaging over radius in k-space, we can obtain a map of all the modes available in the structure as a function of in-plane wave vector. Though not quantitative due to the intensities of the peaks changing with dipole number and position, this method allows for a comparison of the relative density of modes in each structure. This method has recently been used to investigate similar aperiodic structures [15]. Our results are shown in Fig. 9. It is clear that there are additional modes both above and below the air light line for the superlattice case. Though not accessible for light incident on the photonic crystal alone, these additional modes could be excited with the addition of a scattering layer above or below the photonic crystal, as we will show below.

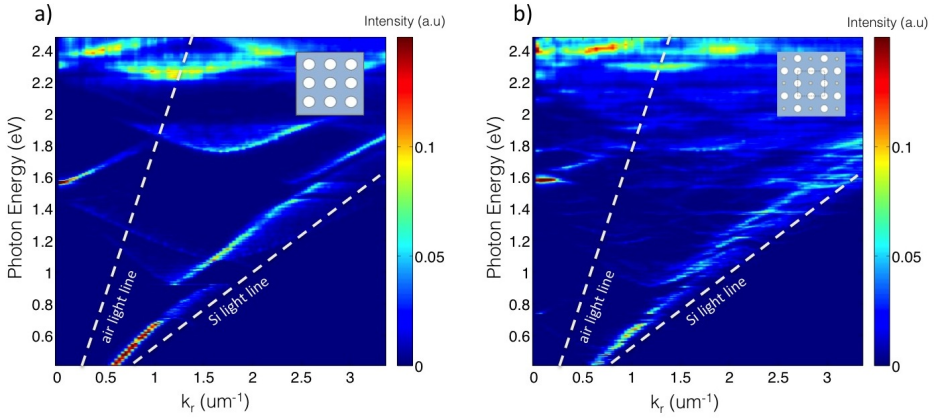

Fig. 9. Maps of available modes as excited by sets of random dipoles in 2D lattice representations of a) base lattice with 290nm period, 232 nm diameter and b) base lattice with 0nm center close packed sublattice. There are clearly new modes introduces both above and below the air light line when the sublattice is added.

#196231 - $15.00 USD Received 22 Aug 2013; revised 5 Nov 2013; accepted 21 Nov 2013; published 3 Dec 2013

3. Superlattices in an optimized hexagonal photonic crystal

The addition of superlattices can be beneficial in many situations. To emphasize this, we now test this concept on a different starting simple periodic lattice. We begin with a hexagonal lattice of air holes in a 200 nm thick slab that has been optimized for absorbed current with respect to lattice constant and air hole diameter. We then introduce a rectangular superlattice on top of the original, forming what is known as a Suzuki lattice [22]. In addition to this, we test one other case by extending the rectangular superlattice into what we term the "extended Suzuki" lattice. Figure 10 shows the spectral absorption for these two cases as we vary the superlattice air hole diameter. Again shown for reference is the original lattice case indicated with a vertical dotted white line. Similar to the square lattice case, increased absorption can be seen on either side of the dotted line at certain wavelengths, corresponding to the introduction of new resonances in the film when the superlattice is introduced. In Fig. 11, we again plot the integrated absorption weighted by the solar spectrum and see that there is again always a superlattice case that outperforms the original lattice. A difference in this case, however, is that the optimum superlattice air hole diameters are not at 0 nm, instead they lie at slightly smaller diameters than the original lattice. The overall enhancement over the original lattice is also less, due to the fact that the starting point was optimized. Nevertheless, a reasonable enhancement is obtained in this case when the optimal superlattice is used. Lastly, in Fig. 12 we calculate the angular response of the original hexagonal lattice and the optimal Suzuki superlattice corresponding to a defect diameter of 210 nm. Again there are many new resonances that are introduced by the addition of the superlattice, leading to increased absorption at all angles.

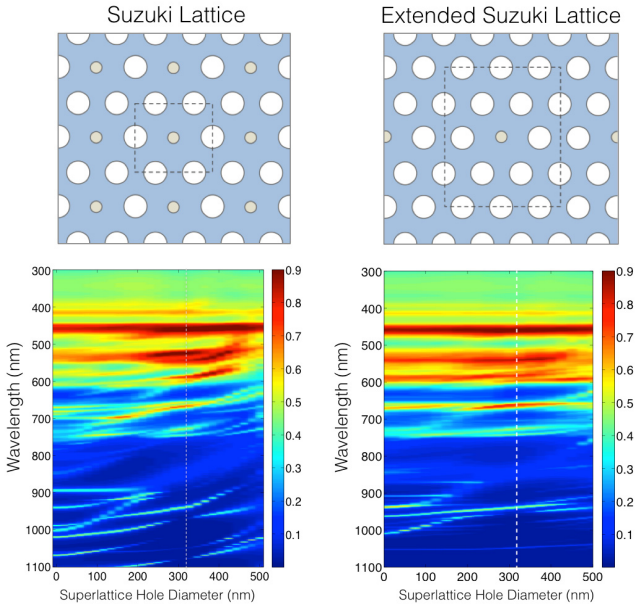

Fig. 10. Fraction of light absorbed at normal incidence for (left) Suzuki lattice and (right) extended Suzuki lattice with a simple periodic lattice of a = 510nm and r = 155nm.

#196231 - $15.00 USD Received 22 Aug 2013; revised 5 Nov 2013; accepted 21 Nov 2013; published 3 Dec 2013

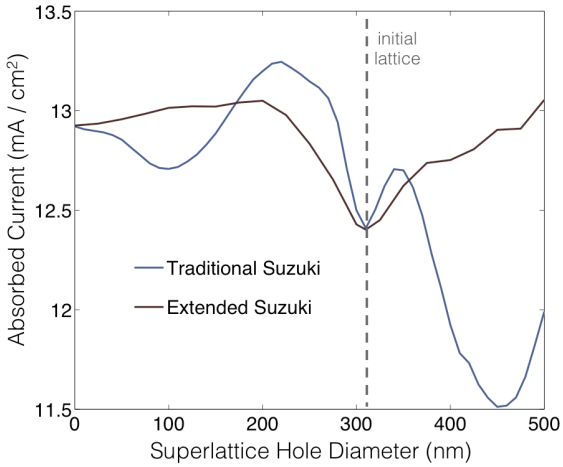

Fig. 11. Absorbed current as a function of superlattice air hole diameter for two different superlattices in the hexagonal lattice obtained by integrating the data in Fig. 9 and weighting by the AM 1.5 solar spectral current.

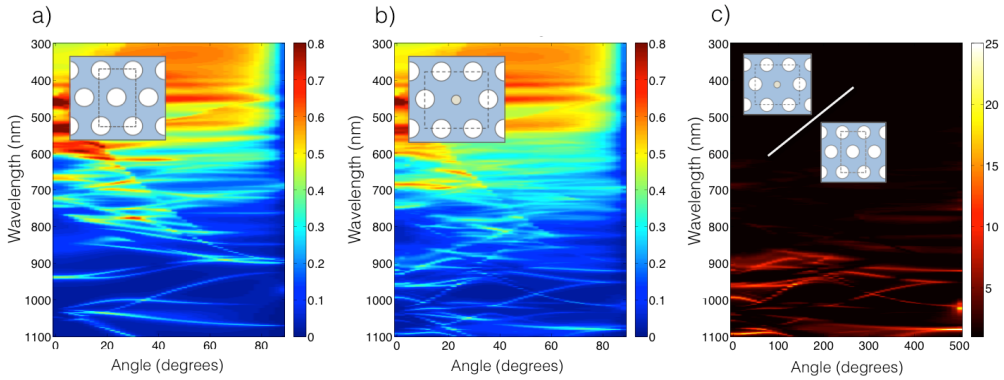

Fig. 12. TE-TM averaged angular absorption spectra for (a) the original hexagonal lattice, (b) the optimal superlattice, and (c) the enhancement ratio.

4. Addition of a randomly textured dielectric incoupler layer

We now further enhance absorption through the addition of a back reflector and a transparent, randomly-textured layer of dielectric material above the absorber. The back reflector adds a second pass for the photons that would otherwise escape out the back of the slab. The randomly textured dielectric incoupler layer enhances anti-reflection as well as helps facilitate randomization of the incoming wavevectors, increasing the number of accessible modes in the slab. We investigated numerous different textures calculated using FDTD at normal incidence. Figure 13 shows the best case we found corresponding to a layer of Si_3N_4 with rms roughness of 40 nm and peak correlation length of 40 nm below a SiO_2 layer with rms roughness of 100 nm and correlation length of 100nm. We typically see an additional ~2 mA/cm^2 of absorbed current due to the back reflector, and in the case of Fig. 13, we see about a 3 mA/cm^2 increase from the randomly-textured dielectric incoupler. This leads us to a total absorbed current of 18.3 mA/cm^2 for the initial square lattice in this study with a = 290 nm and d = 232 nm. When this same texturing is placed on the optimal hexagonal superlattice case (a = 510 nm, d = 310 nm, $d_{superlattice}$ = 210 nm) we achieve a absorbed current of 19.5 mA/cm^2. Additionally, when we start with a different square lattice with optimized period and air hole diameter (a = 550 nm, d = 350 nm) and add an optimized edge close-

#196231 - $15.00 USD Received 22 Aug 2013; revised 5 Nov 2013; accepted 21 Nov 2013; published 3 Dec 2013

packed superlattice ($d_{superlattice}$ = 300 nm), as well as a randomly-textured dielectric incoupler, we observe the highest absorbed current of this study at 20.7 mA/cm^2. This is still less than the ergodic limit at 200 nm total thickness which is ~31 mA/cm^2. If we instead use the equivalent thickness of our structure, which is 144 nm, the optimal structure is closer but still below the ergodic limit at this thickness of ~29mA/cm^2. While a different structure may be necessary to reach or exceed the ergodic limit, the absorbed current of 20.7 mA/cm2 is still more than 2 times larger than that of a planar Si slab with the same roughened texturing at 9.96 mA/cm^2, as shown in Fig. 13. We have also confirmed that each of the optimized superlattice structures have higher absorbed currents than the same randomly-textured dielectric incoupler applied to each of their respective starting lattices. These higher currents are achieved with the same incoupler due to the greater number of modes in the optimized superlattice than both the planar slab and the starting lattice.

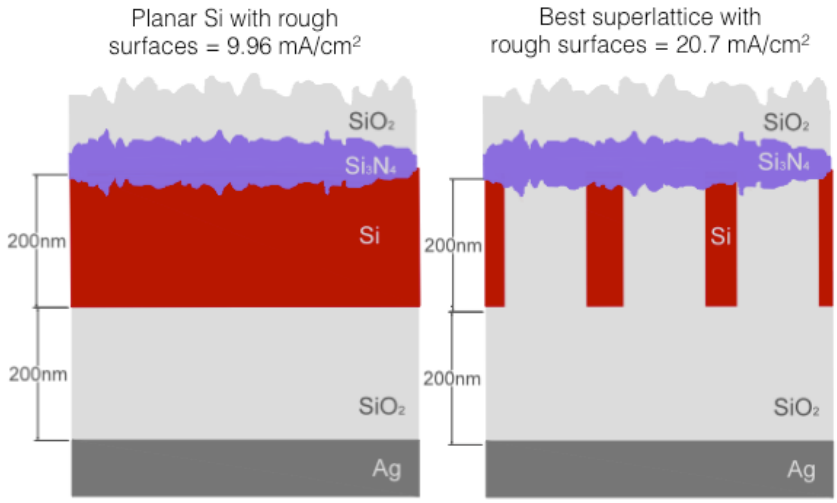

Fig. 13. Schematic of a planar slab with roughened texturing (left) and the highest-performing structure (right), wherein a photonic crystal superlattice is integrated with a randomly textured dielectric incoupler.

5. Thicker absorber layers

The previous calculations were all done for 200 nm thick Si slabs mainly to illustrate the effects of different light trapping strategies. For thin layer Si cells to be competitive with commercial Si photovoltaic efficiencies, slightly thicker active regions and higher currents are necessary. To show that our approach can be extended to thicker absorbing regions, we simulated superlattice photonic crystal layers with randomly-textured dielectric incouplers with Si thicknesses of 1 to 4 microns, which can result in absorbed currents between 30 and 40 mA/cm^2. For example, our 2 um thick cell has ~34 mA/cm^2, comparable to other results in the literature [23] with similar thicknesses. It is also worth noting that we do not use equivalent thickness as a metric as it can complicate comparison of different patterns. These currents are not only approaching the ergodic ray optic light trapping limit for these thicknesses, but also show that our designs may be implemented to create thin film cells that are competitive in efficiency with thicker cells. In Fig. 14 we show the simulated maximum absorbed currents for different geometries and thicknesses ranging from 200nm to 4 microns and compare with the ergodic limit.

#196231 - $15.00 USD Received 22 Aug 2013; revised 5 Nov 2013; accepted 21 Nov 2013; published 3 Dec 2013

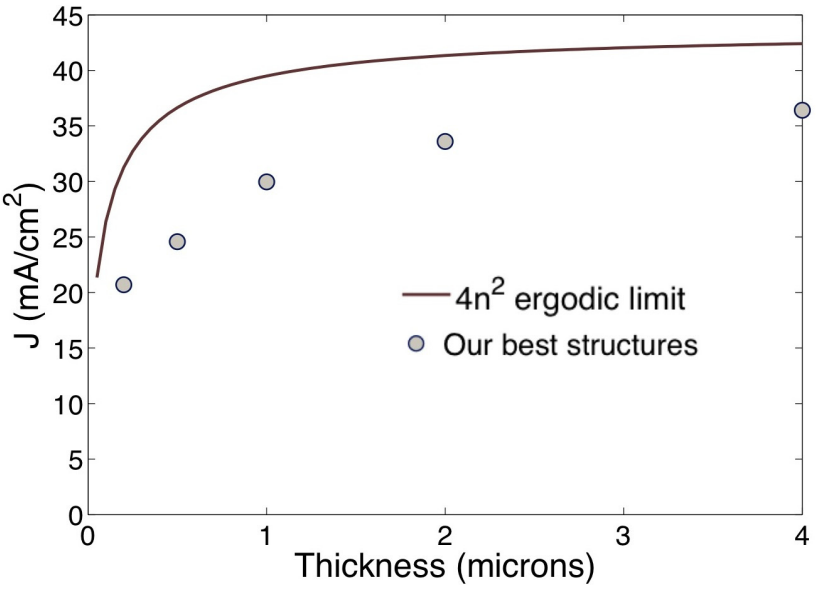

Fig. 14. Summary of the change in absorbed current with changes in the geometry and thickness of the absorbing layer compared to the ergodic light trapping limit.

5. Conclusions

These results strongly suggest that simple periodic lattices are not optimal for light trapping in photonic crystals and that incorporation of additional superlattices can significantly increase absorption at all angles. Also, these results indicate that finding optimal disorder is not always trivial, as evidenced by the fact that the optimal superlattice type and diameter was different for different starting lattices. Thus, large multiparameter optimizations may be necessary to find optimal light trapping structures incorporating disorder. We have just provided one example of combining periodic and random structures to increase light trapping, but do not claim to have found an absolute best combination. Much more work is needed to fully explore the other regions of the periodic to random continuum depicted schematically in Fig. 1. Two obvious extensions of the superlattice structures we have studied would be to introduce defects at non-periodic sites in a photonic crystal lattice and to use a polydisperse size distribution of defects. These scenarios are much more computationally demanding and thus were not explored in this work, but will be the subject of future work. We have also shown that the combination of superlattice photonic crystals with randomly-textured dielectric incouplers significantly increases absorption. This is due to the fact that rough surfaces randomize incoming photons, lifting the constraint of selective mode occupation that occurs with periodic structures. These findings lend support to the idea that for most light trapping applications, a combination of periodic and random texturing may be optimal.

Acknowledgments

D. M. C. acknowledges the Department of Energy Basic Energy Sciences, Office of Science through the 'Light Material Interactions Energy Frontier Research Center' under contract number DE-SC0001293. K. A. W. H. acknowledges the Bay Area Photovoltaic Consortium under award number DE-EE0004946 and a graduate research fellowship from the National Science Foundation.

#196231 - $15.00 USD Received 22 Aug 2013; revised 5 Nov 2013; accepted 21 Nov 2013; published 3 Dec 2013